Wettability of End-Grafted Polymer Brush by Chemically Identical Polymer Films

Xueyun Zhang,[†] Fuk Kay Lee,[‡] and Ophelia K. C. Tsui*,[‡]

Department of Chemical and Biomolecular Engineering, Hong Kong University of Science and Technology, Clear Water Bay, Hong Kong, and Department of Physics, Boston University, Boston, Massachusetts 02215

Received July 9, 2008; Revised Manuscript Received August 14, 2008

ABSTRACT: Previous experiments on chemically homogeneous polymer melt−brush systems have found large deviations from theory. By using X-ray reflectivity and atomic force microscopy, we find that the equilibrium structure of these systems is complex, composed of dewetted droplets of the constituent polymers residing on a residual film of the end-grafted brush swollen by the free melt chains. When the molecular weight of the melt or the grafting density of the brush is decreased, the thickness of the residual film increases and the contact angle decreases, both indicating improved wettability. At the same time, the profile of the dewetted droplets exhibits a progressively longer and gentler tail at the ends. But a wetting−dewetting transition is never observed. By comparing the measurements to recent results of the self-consistent field theory, good quantitative agreement is found. On the other hand, Leibler's analytical theory—which has been used almost exclusively for comparison with experiment—provides a poor description.

Introduction

It is a daily experience that a liquid drop wets the surface of the same liquid. But an end-grafted layer of polymer brush may dewet a chemically identical polymer film. This phenomenon, known as autophobic dewetting, primarily arises from the loss of configurational entropy of the polymer chains in the film when put in contact with the brush.[1−6] Evidence to the entropic origin of the melt−brush interface has been found by Reiter and Khanna who showed that the effective interfacial energy, $\gamma^{\mathrm{eff}}_{\mathrm{MB}}$, as determined from the contact angle of the dewetted droplets, increased in direct proportion to the specimen's temperature, T, i.e., $\gamma^{\mathrm{eff}}_{\mathrm{MB}} = +T|\Delta S|$, where ΔS is the excess entropy of the melt−brush interface.[7] This finding suggests that ΔS is *negative* and the compatibility between the brush and the melt deteriorates with increasing T. This is in contrast with the temperature dependence, $\Delta H - T\Delta S$, typically found among interfaces between two polymers (ΔH is the unit-area change in enthalpy upon contact), where the second term, $-T\Delta S$ is usually negative, leading to the prevailing observation that the miscibility between two polymers usually improves with increasing T.

Alias the entropic origin of autophobicity in homogeneous polymer melt−brush systems is well-known, attempts to account for the magnitude of the observed contact angle of the dewetted droplets[1,7] have found an order of magnitude disagreement with Leiber's strong-stretching theory (SST),[1] which is based on the loss of configurational entropy of a strongly stretched polymer brush solvated by a matrix of chemically identical polymer melt and the gain in the translational entropy of the latter. The SST leads to analytical expressions for the excess energy and interfacial width of the melt−brush interface. Leibler et al.[1] suggested that the discrepancy could arise from viscoelastic deformations of the brush layer occurring when the dewetted droplets receded on top, which resulted in modifications to the profile of the droplets (see Figure 1). On the other hand, Matsen[5] pointed out that the treatment of the SST in ref 1 was in fact inadequate, leading to results inconsistent with that of the self-consistent field theory (SCFT).[2,5,6,8] In this paper, we report detailed characterization of the interfacial properties of a polystyrene (PS) melt−brush model system, including the equilibrium melt−brush film thickness, contact angle of the dewetted droplets, and the droplet profile. Altogether, these measurements allow the SCFT to be critically evaluated. Our result shows that the SCFT provides a good comprehensive description of the experiment.

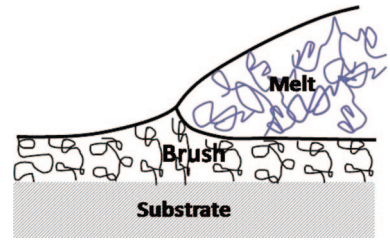

Figure 1. Picture proposed in ref 1 depicting how viscoelastic deformations may explain the discrepancy between the contact angle found in autophobic experiments and the prediction by SST.

Experimental Details

Sample Preparation. We adopt the "graft to" method in making the polymer brush.[9] Previous study using a block copolymer for the brush material found that the free melt chains often penetrate more than one lamellae period into the block copolymer layer and effectively destroy the presumed "brush" structure.[10] Here, we use monohydroxy-terminated polystyrene with weight-average molecular weights $M_w^{\mathrm{PSOH}} = 24$ and 52.5 kg/mol (hereafter denoted PSOH24k and PSOH52k, respectively) and polydispersity ≤ 1.04 to be the brush materials, which had been purchased from Polymer Source Inc. The substrates are silicon covered by a 5 nm thick oxide and cleaned as described before.[11] A solution of the brush polymer in toluene is spun-cast onto the substrates after cleaning. The resulting films are annealed at 170 °C under 10^{-3} Torr for 24 h. The brush chains unreacted with the substrates are removed by thorough rinsing of the annealed films in toluene. Monodispersed homopolystyrene (HPS) with various molecular weights ($24.7 \leq M_w^{\mathrm{HPS}} \leq 393.4$ kg/mol and polydispersity between 1.03 and 1.2), some purchased from Polymer Source Inc. and some from Scientific Polymer Product, are dissolved in toluene before being spun-cast

* Corresponding author. E-mail: okctsui@bu.edu.
[†] Hong Kong University of Science and Technology.
[‡] Boston University.

10.1021/ma801549r CCC: $40.75
Published on Web 10/07/2008

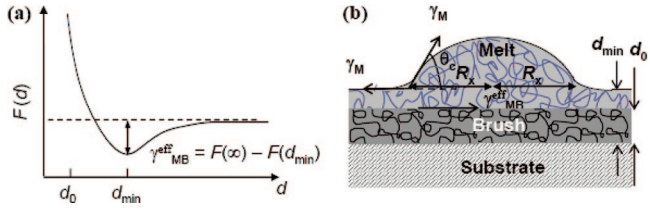

Figure 2. (a) Sketch of a generic (unit-area) interfacial potential of a polymer melt−brush system according to the SCFT result. (b) Illustration of how the parameters of the interfacial potential, d_0 and d_{min}, shown in (a) are connected to the characteristic features of a droplet dewetted from a polymer melt−brush system.

onto the previously prepared brush films to form the specimens. The melt−brush specimens are allowed to dewet at 170 °C in nitrogen for 12 h, whereupon the HPS on the brush disintegrate into isolated droplets.

Experimental Techniques. *X-ray Reflectivity.* X-ray reflectivity measurements were performed with the model PW1825 high-resolution X-ray diffractometer (XRD) system by Philips Analytical (Almelo, The Netherlands). This XRD system is quipped with a 2 kW Cu rotating anode X-ray source ($\lambda = 1.54$ Å) and a four-crystal monochromator ($\Delta\lambda = 0.000461$ Å) for high-resolution analysis. The equilibrium melt−brush thickness and the brush thickness were determined by fitting the XR curves to a trilayer model PS−SiO_2−Si: The brush and any homopolymer melt on top were modeled as one single PS layer. In the fitting procedure, the electron densities of PS, SiO_2, and Si were kept constant while the thicknesses and roughness of PS and SiO_2 were allowed to vary. The roughness for most samples obtained through the fitting is within 1 Å. The droplet profiles of dewetted droplets were captured by a Seiko Instrument SPN3800 atomic force microscope (AFM) operated in the noncontact mode.

Results and Discussion

The grafting density of the brush, σ, is determined by $\sigma = \rho d_0 N_A / M_w^{PSOH}$, where ρ is the mass density of the brush, N_A is Avogadro's number, and d_0 is the thickness of the brush when it is "dry", i.e., free of any melt or unbound brush chains. The thickness of most of the HPS cast films is 16 nm. We found no visible change to the result when the HPS thickness was increased to 32 nm or other thicknesses in between. An important result of the SCFT is that the (unit-area) melt−brush interfacial potential, $F(d)$, possesses a minimum at a finite thickness, d_{min}, and approaches zero as d approaches infinity (Figure 2a). With this, the specimen after dewetting should form a residual film with thickness equal to d_{min}. The thickness of the residual film and the dry thickness of the brush were obtained by fitting the X-ray reflectivity curves with the three-layer model PS−SiO_2−Si.[12]

Because of its entropic origin, γ^{eff}_{MB} is usually much smaller than the surface tension of the polymer, γ. Correspondingly, the maximum gradient of the droplets has been found to be $< \sim 0.1$ rad here. With the spatial extent of the interfacial potential, $F(d)$, being of the order of the gyration radius of the brush polymer ($\sim$10 nm here),[2,6] the lateral extent of the droplet under the influence of $F(d)$ is >100 nm. This leads to a measurable tail in the profile of the dewetted droplets (Figure 2b). Consider a droplet with dimensions much smaller than the capillary length (approximately millimeter). The gravitational potential energy is negligible compared to γ, so the profile of an axisymmetric droplet (namely, $d = d(r)$) is governed by the following Young−Laplace equation (which simply expresses that the normal stress is zero at the liquid−air interface):

$$\frac{dF(d)}{dd} = \gamma\left[\frac{r d_{rr}}{r(1+d_r^2)^{3/2}} + \frac{d_r(1+d_r^2)}{r(1+d_r^2)^{3/2}}\right] \quad (1)$$

where r is the radial distance measured from the center of the droplet. Because d_r is <0.1 as mentioned above, $1 + d_r^2 \approx 1$. Moreover, because the footprint radius of the droplet, R_x (which is >5 μm) is much larger than the lateral extent of the interfacial potential (<0.2 μm here), the second term in eq 1 can be ignored. The resultant equation, $F'(d) = \gamma d''(r)$ has the same form as that deduced for a one-dimensional droplet in Cartesian coordinate and has the solution[6]

$$[d'(x)]^2 = 2[F(d(x)) - F(d(x_{min}))]/\gamma \quad (2)$$

or

$$d(x) = d_{min} + \int_0^x dx \sqrt{\frac{2}{\gamma}[F(d(x)) - F(d(x_{min}))]} \quad (3)$$

where the coordinate x has been so chosen that $d(x=0) = d_{min}$. Equation 3 is valid up to the point where the $F(d(x)) = 0$ asymptotic behavior just begins. Beyond this point, the droplet profile is spherical with a radius of curvature, $R \approx R_x/\sin\theta_C$, where θ_C is the angle subtended by the droplet at that point; it is also the maximum angle subtended by the droplet to the substrate (see Figure 2b). By eq 3, $\tan\theta_C = (2\gamma^{eff}_{MB}/\gamma)^{1/2}$, where $\gamma^{eff}_{MB} \equiv F(\infty) - F(d_{min})$, namely, the depth of the potential minimum (Figure 2a). For small θ_C, this relation is the same as Young's equation given that θ_C is the contact angle and the residual film has the same surface tension, γ, as the liquid. The angle, θ_C is thus referred to as the contact angle. In this experiment, we deduce θ_C from the profile of the dewetted droplets captured by tapping-mode AFM.

To enable comparison between results obtained from specimens made of different molecular weight brush polymers, we normalize all the thicknesses by the gyration radius of the brush, $N_B^{1/2}a$ (where N_B is the degree of polymerization of the brush polymer, a is the statistical length, and ρ_0^{-1} is the volume of a chain segment) and volumes by the pervasive volume of a brush chain, $N_B\rho_0^{-1}$. Correspondingly, grafting densities (≡ the number of grafted brush chains per unit area) are normalized by $N_B^{-1/2}a\rho_0$.

Figure 3 shows the X-ray reflectivity curves (solid circles) from a series of dewetted specimens made of the PSOH24k brushes with the same initial thickness of 11.4 nm, but the HPS melt polymer has different molecular weights ($\alpha = M_w^{HPS}/M_w^{PSOH}$ is from 1.4 to 8.9). As seen, the Kiessig fringes are clearly discernible and the XR curves can be well fitted to the model consisting of a PS−SiO_2−Si trilayer (solid lines). This result indicates that the (incoherent) scatterings from the dewetted droplets make negligible contribution to the XR signal and the features in the XR curves come essentially from the residual film underneath. It is important to note that most of the measured residual film thicknesses (= d_{min}) are smaller than the initial thickness of the brush. Therefore, some of the brush chains must have come off during annealing. To determine the actual dry thickness, d_0, of the brush, we rinse the specimen with fresh toluene to remove the unbound brush chains and the free HPS. X-ray reflectivity reveals that $d_0 = 8.5 \pm 0.4$ nm or a normalized grafting density, $\sigma' = 0.84 \pm 0.04$. Increasing the initial thickness of the HPS by a factor of 2 does not produce any noticeable change to the value of d_0, suggesting that the brush chains that have come off have negligible effect on the equilibrium of the melt−brush system. In addition, further annealing of the melt−brush films at 170 °C up from 12 to 118 h produces less than 0.3 Å change to the values of d_0 and d_{min} (Figure 4), indicating that the melt−brush system is very close to, if not already at, equilibrium within the typical annealing time of 12 h. Figure 3 also shows that the equilibrium

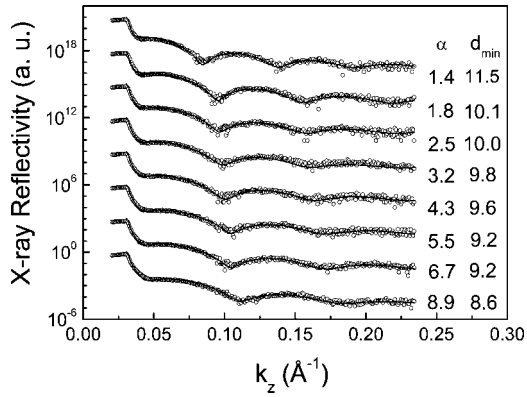

Figure 3. X-ray reflectivity curves of a series of dewetted melt−brush specimens with various values of $\alpha = M_w^{HPS}/M_w^{PSOH}$ on PSOH24k brushes with the same initial thickness of 11.4 nm. The abscissa is the component of the incident X-ray wave vector normal to the film. The data have been shifted vertically for clarity. The residual thicknesses, d_{min}, deduced by curve-fitting with the Parrat formulism assuming a three-layer model (PS−SiO_2−Si) (ref 12) are as shown. The solid lines are the fitted curves. The curve with $\alpha = 8.9$ is the original data. Successive curves are offset by a factor of 1000 for clarity.

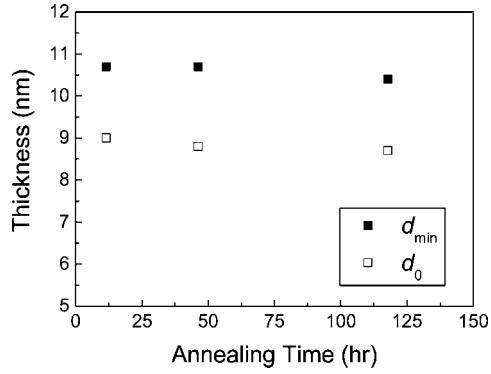

Figure 4. Measured values of d_{min} and d_0 as a function of annealing time at 170 °C of specimens with $\alpha = 1.84$ on a PSOH24k brush, where the initial thicknesses of the melt−brush specimens are the same, equal to 11.4 nm.

melt−brush thickness, d_{min}, decreases with increasing α. This observation is consistent with both scaling analysis[13] and the SCFT.[14] In a matrix of chemically identical molten polymer, the brush chains stretch normal to the substrate due to the excluded volume effect of the polymer molecules, which act as a good solvent. As the molecular weight of the molten polymer increases, the excluded volume effect becomes progressively screened and the stretching of the brush chains diminishes, which provides a physical explanation to the data of Figure 3.

Shown in Figure 5 are the data of the equilibrium thickness of the melt−brush specimens made of the PSOH24k (solid symbols) and PSOH52k (open symbols) brushes with different normalized grafting densities, σ', from 0.28 to 0.84. The data are displayed as the normalized thickness of the free melt in the residual film, i.e., $(d_{min} - d_0)/N_B^{1/2}a$, versus α. As seen, the data obtained from specimens made of the two different brush materials collapse quite well. Moreover, good agreement between the measurement and the SCFT prediction[6] (continuous lines) is apparent. The slight deviation seen in the region of large α could arise if the dry thickness of the brush films had been underestimated. When the dewetted melt−brush specimens are rinsed in toluene to reveal the actual dry thickness of the brush, the toluene swells both the melt and the brush. Before all the (swollen) melt chains are expelled from the brush, a large strain can develop inside the brush causing some brush chains

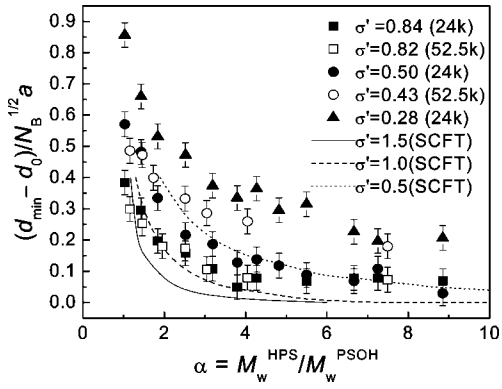

Figure 5. $(d_{min} - d_0)/N_B^{1/2}a$ plotted as a function of α for various normalized grafting densities as shown. Continuous lines are the SCFT predictions reproduced from ref 6. Solid and open symbols denote data of specimens made of the PSOH24k and PSOH52k brush, respectively.

to come off. Because the degree of swelling or stretching of the brush is bigger with bigger molecular size of the melt polymer and/or longer brush chains,[9,13] this effect is stronger for specimens with larger α and/or M_w^{PSOH}, which is in keeping with the corresponding bigger deviations found in Figure 5 between theory and experiment. The data of Figure 5 shows that for the same M_w^{HPS}, $(d_{min} - d_0)/N_B^{1/2}a$ is bigger for brushes with a lower grafting density. And, for the same grafting density, $(d_{min} - d_0)/N_B^{1/2}a$ decreases steadily with increasing M_w^{HPS}. Previously, Oslanec et al.[15] reported a stretched to nearly collapsed transition of dPS-*b*-PMMA block copolymer chains adsorbed from a HPS matrix to a silicon oxide surface as the molecular weight of the HPS was increased. The present data shows that such transition takes place only in specimens where $\sigma' > \sim 1$. We also observe that $(d_{min} - d_0)/N_B^{1/2}a$ varies smoothly with α showing no obvious sign of wetting−dewetting transition, deviant from previous suggestions.[1,8,10,16,17]

We next examine the effective melt−brush interfacial energy, γ^{eff}_{MB}, deduced from specimens made of PSOH24k brushes with $\sigma' = 0.5$, 0.72, and 0.84, but different M_w^{HPS}. The data are displayed as γ^{eff}_{MB} versus α in Figure 6a. As seen, the measured γ^{eff}_{MB} generally increases with increasing M_w^{HPS}. For the same M_w^{HPS}, γ^{eff}_{MB} is bigger for specimens with a bigger grafting density. All these demonstrate good consistency with the SCFT (continuous lines). However, the data are consistently larger than the SCFT predictions by 50−100% though we note that the deviations from those of the SST are more than 5 times worse (inset of Figure 6a). The deviations noted here with the SCFT for the value of γ^{eff}_{MB} are in fact consistent with an underestimation of the dry thickness of the brush and hence its grafting density proposed above. This interpretation is also in line with the observation that the deviations get bigger for specimens with bigger σ' where the strain developing in the brush during swelling should be larger. Below $\alpha \approx 3$, the $\sigma' = 0.5$ experimental data depart somewhat from the theory, with the values of γ^{eff}_{MB} remaining finite at ~0.015 mJ/m^2 near $\alpha = 1$, whereas the theory predicts that it should level off to zero. Since the same order of contact angle hysteresis had been found during the dewetting of a poly(dimethylsiloxane) melt−brush model system,[7] our observation can arise from pinning at the contact line of the droplets caused by heterogeneity of the melt−brush interface.

We have also examined the profiles of the droplets dewetted from specimens made of the PSOH24k brushes with the same $\sigma' = 0.84$, but HPS with different values of α. The results are shown in Figure 6b for the region magnified around the contact line (symbols). Because the contact angles of the droplets are small (≤7°) compared to the complement of the half-cone angle

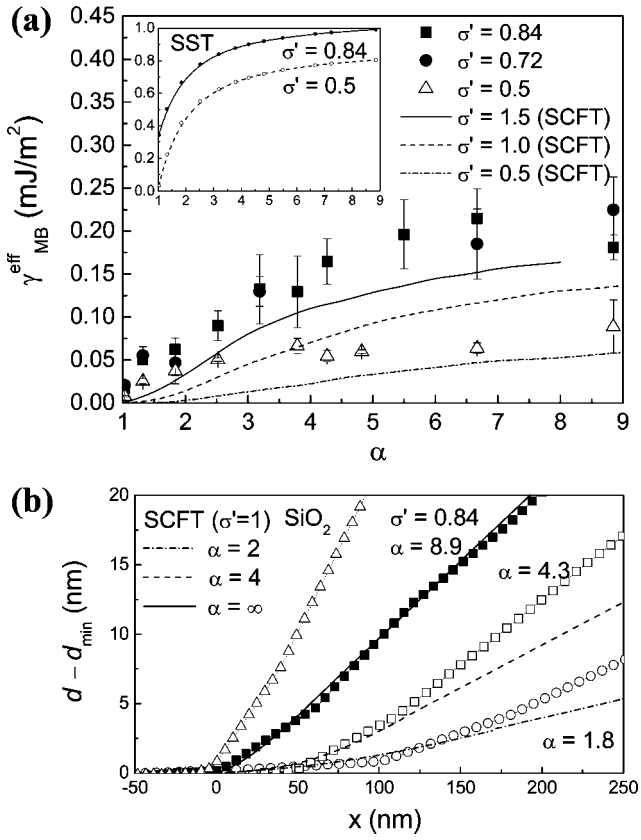

Figure 6. (a) γ^{eff}_{MB} plotted vs α for specimens made of PSOH24k brushes with different normalized grafting densities, σ', indicated. The continuous lines denote the SCFT predictions reproduced from ref 6. Inset: Calculations based on the SST (refs 1 and 6). (b) Profiles of the dewetted droplets with α = 1.8 (■), 4.3 (□), and 8.9 (○) on PSOH24k brushes with $\sigma' = 0.84$. The profile of a droplet of HPS (M_w = 24 kg/mol) dewetted from a bare substrate is also shown (Δ). Smooth lines are the model profiles described in the text.

of the AFM tip, which is ∼15°, the measured profile should replicate the actual profile quite well. This was confirmed by performing deconvolution of the droplet profiles by the tip radius (= 10 nm) and finding that the calculated profiles overlap with the measured profiles within scatter of the data (data not shown). According to Figure 6b, as α increases, the contact angle increases and the spatial extent of the tail of the droplet decreases. The profile of a HPS droplet dewetted from a bare substrate is also shown (open triangles). As seen, it rises notably more abruptly above the contact line than the other droplets do, indicating that the van der Waals potential and enthalpic interactions between homopolymer and the substrate, which pertains when the brush layer is absent, has a much shorter range of interaction than the brush thickness. The smooth lines are model curves calculated by using eq 3 and the data of $F(d)$ published in ref 6. Good consistency between the model and experimental profiles is apparent. The discrepancies seen for the α = 1.8 and 4.3 droplets in the large x region originates from the corresponding discrepancies found in γ^{eff}_{MB} (Figure 6a) discussed above.

Conclusion

In conclusion, we have studied in detail the autophobicity of a model PS melt−brush system by measuring the equilibrium thickness and contact angle of the specimens as a function of a broad range of melt-to-brush molecular weight ratio ($1 \le \alpha \le 8.9$) for various fixed grafting densities of the brush. We have also measured the profiles of HPS droplets dewetted from specimens at various α, but the same grafting density. A comprehensive comparison between the measurements and the predictions of SCFT (notably those published in ref 6) demonstrates an order of magnitude improvement in the agreement between theory and experiment on the autophobicity of polymer melt−brush systems. Moreover, the specificities displayed by our data, being in excellent accord with the SCFT (Figures 5 and 6), also undermine the viscoelastic effect proposed by Leibler et al. (Figure 1) in explaining the discrepancy between experiment and their theory.[1]

Acknowledgment. We are indebted to Mark Matsen for valuable discussions and his sending us the data of $F(d)$ published in ref 6. O.K.C.T. is grateful for the support of the NSF (Project No. DMR-0706096) and the ACS Petroleum Research Fund (Project No. 47882-AC 5).

References and Notes

(1) Leibler, L.; Ajdari, A.; Mourran, A.; Coulon, G.; Chatenay, D. Presented at the *OUMS Conference on Ordering in Macromolecular Systems*, 3–6 June, 1993, Osaka, Japan.
(2) Shull, K. R. *Faraday Discuss.* **1994**, *98*, 203–219.
(3) Kerle, T.; Yerushalmi-Rozen, R.; Klein, J. *Macromolecules* **1998**, *31*, 422–429.
(4) Voronov, A.; Shafranska, O. *Langmuir* **2002**, *18*, 4471–4477.
(5) Matsen, M. W. *J. Chem. Phys.* **2005**, *122*, 144904–8.
(6) Matsen, M. W.; Gardiner, J. M. *J. Chem. Phys.* **2001**, *115*, 2794–2804.
(7) Reiter, G.; Khanna, R. *Phys. Rev. Lett.* **2000**, *85*, 5599–5602.
(8) Ferreira, P. G.; Ajdari, A.; Leibler, L. *Macromolecules* **1998**, *31*, 3994–4003.
(9) Chen, W. Y.; Zheng, J. X.; Cheng, S. Z. D.; Li, C. Y.; Huang, P.; Zhu, L.; Xiong, H.; Ge, Q.; Guo, Y.; Quirk, R. P.; Lotz, B.; Deng, L.; Wu, C.; Thomas, E. L. *Phys. Rev. Lett.* **2004**, *93*, 028301.
(10) Liu, Y.; Rafailovich, M. H.; Sokolov, J.; Schwarz, S. A.; Zhong, X.; Eisenberg, A.; Kramer, E. J.; Sauer, B. B.; Satija, S. *Phys. Rev. Lett.* **1994**, *73*, 440–443.
(11) Tsui, O. K. C.; Wang, Y. J.; Lee, F. K.; Lam, C.-H.; Yang, Z. *Macromolecules* **2008**, *41*, 1465–1468.
(12) Tsui, O. K. C.; Russell, T. P.; Hawker, C. J. *Macromolecules* **2001**, *34*, 5535–5539.
(13) De Gennes, P. G. *Macromolecules* **1980**, *13*, 1069–1075.
(14) Zhulina, E.; Boisov, O. V.; Brombacher, L. *Macromolecules* **1991**, *24*, 4679–4690.
(15) Oslanec, R.; Vlcek, P.; Hamilton, W. A.; Composto, R. J. *Phys. Rev. E* **1997**, *56*, R2383−R2386.
(16) Maas, J. H.; Fleer, G. J.; Leermakers, F. A. M.; Stuart, M. A. C. *Langmuir* **2002**, *18*, 8871–8880.
(17) Jopp, J.; Yerushalmi-Rozen, R. *Macromolecules* **1999**, *32*, 7269–7275.

MA801549R